National Aeronautics and Space Administration
Ames Research Center • Entry Systems and Technology Division

Defining the Operational Envelope for Air Flows in the miniature Arc-jet Research Chamber (mARC II)

Jocelino Rodrigues[1], Megan E. MacDonald[2], Magnus A. Haw[2], Ramon Martinez[2], Daniel Philippidis[2], Sebastian Colom[3], Ryan Chung[4], Joe Hartman[4]

[1]NASA Postdoctoral Program at NASA Ames Research Center
[2]NASA Ames Research Center
[3]AMA Inc. at NASA Ames Research Center
[4]Sierra Lobo Inc. at NASA Ames Research Center

CREATED AT NASA AMES RESEARCH CENTER, MOFFETT FIELD, CALIFORNIA 94035-1000.
PRESENTED AT THE AIAA AVIATION FORUM, LAS VEGAS, NEVADA, USA, JULY 29–AUGUST 2, 2024.
GT-02: ARC-JET FACILITY DEVELOPMENT AND CHARACTERIZATION

Motivation

Supporting the development and testing of low-maturity level technologies

NASA Ames has a strong legacy in ground-testing:

- Operates six high-power arc-heaters (10–60 MW) to deliver high-enthalpy flows (convective and/or radiative) for extended periods of time and for various gas mixtures
- Relied upon for every NASA mission with entry phase

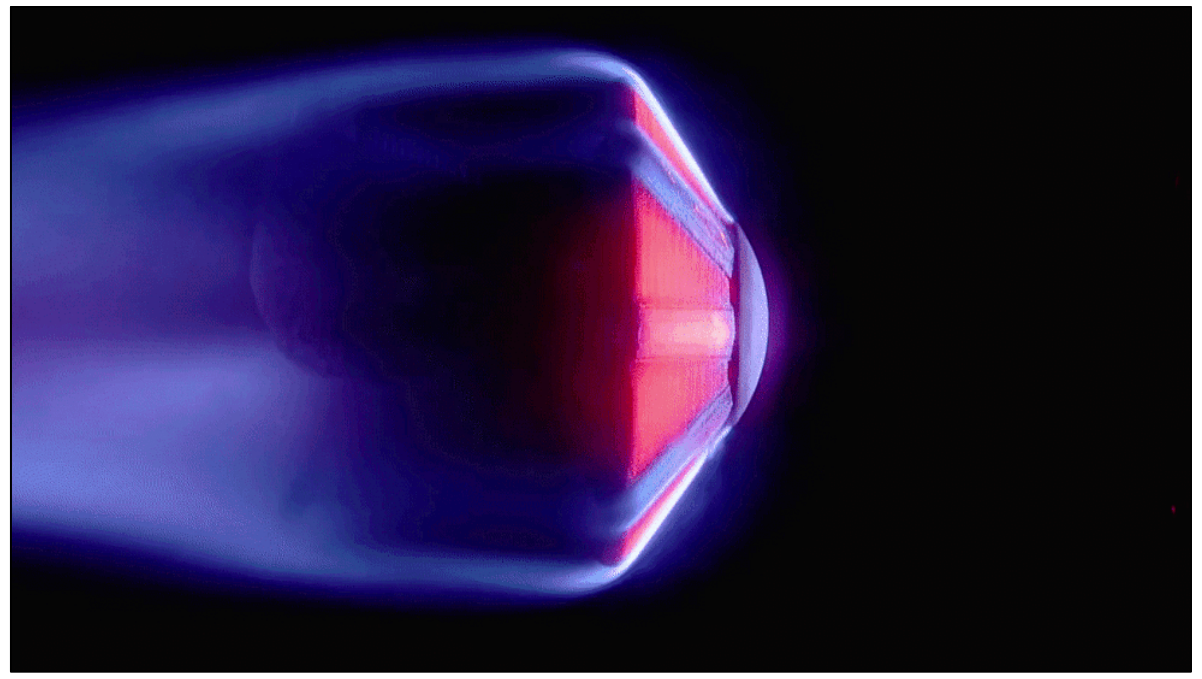

ADEPT arc-jet test – 60 MW IHF
Credit: NASA/TSF

Demand for a smaller-scale facility to support the rapid, low-cost development of low-maturity technologies prior to them being implemented/tested in the larger facilities:

- Diagnostics (e.g., non-intrusive flow measurements)
- Instrumentation (e.g., intrusive flow measurements)
- Materials (e.g., screening of novel TPS)

mARC II's previous vacuum system was unable to maintain $p_e/p_\infty>1$ under test conditions

100 A, 0.25 g/s

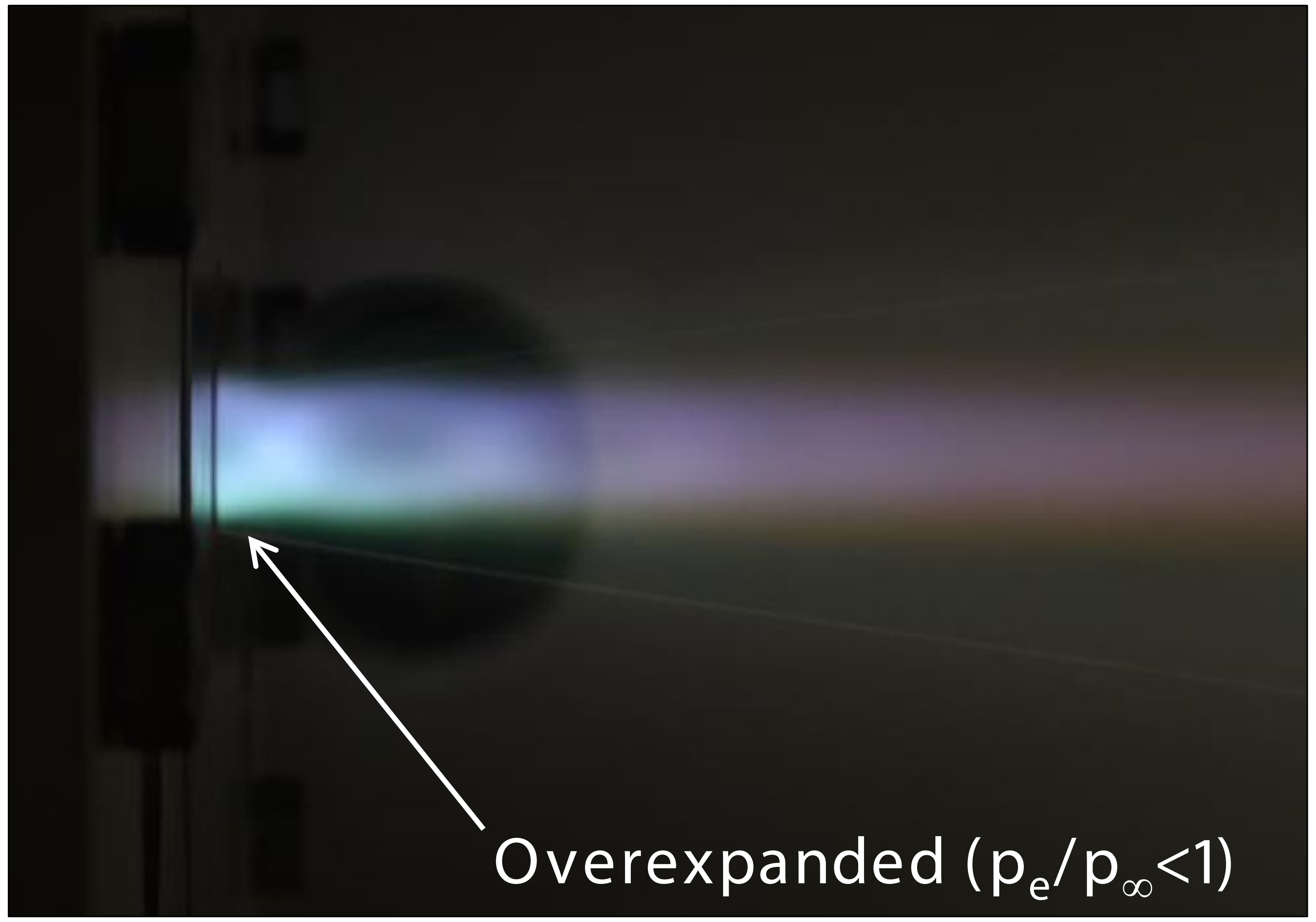

100 A

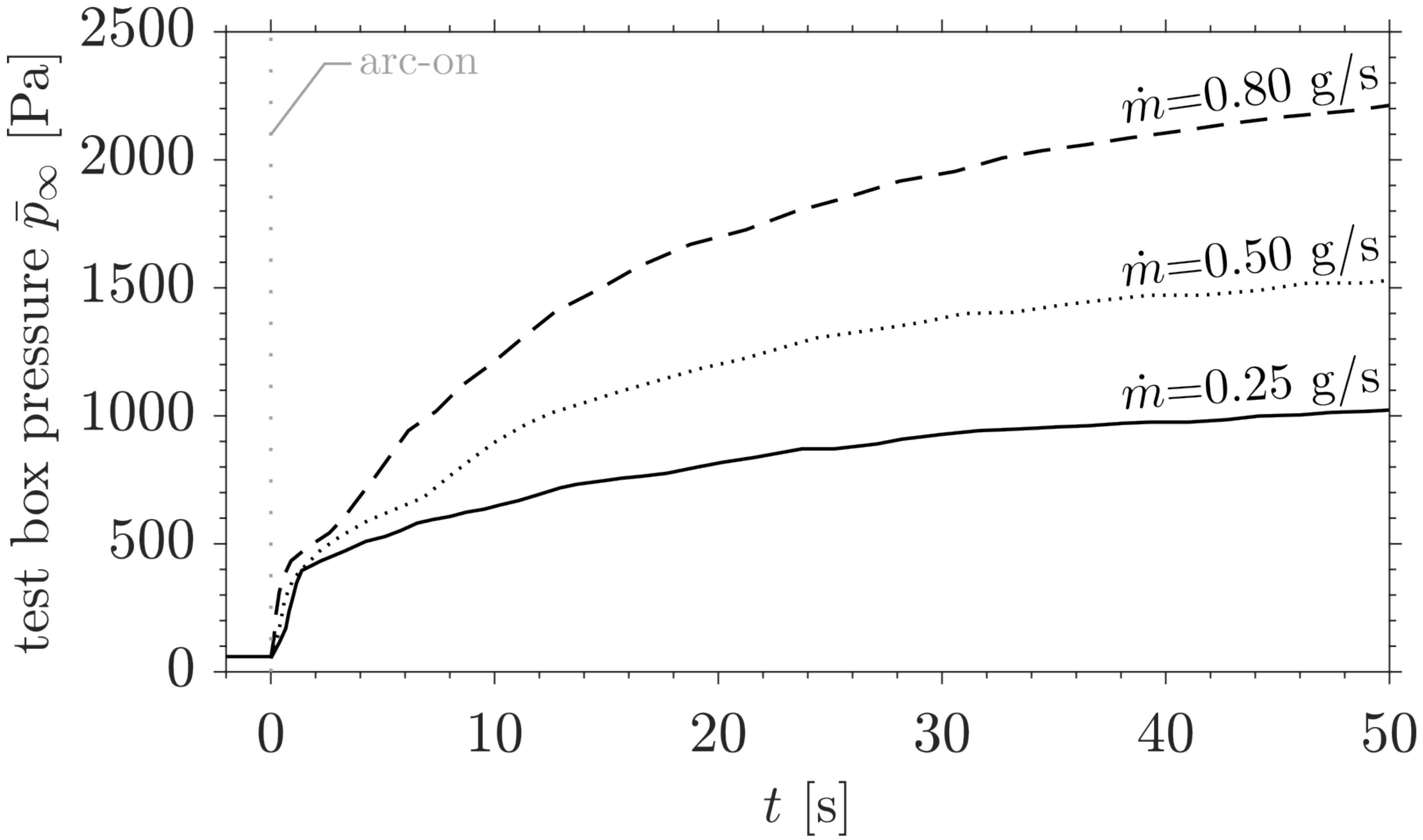

- Underexpanded flow ($p_e/p_\infty>1$) is desirable to provide large region of constant flow conditions.
- High test box pressures after arc-on were the root cause of overexpanded flow ($A/A^*\simeq 11.3$).
- To reliably sustain $p_e/p_\infty>1$, the need for a new vacuum system was identified.

mARC II

miniature Arc-jet Research Chamber (second-generation)

Facility — arc heater & test box

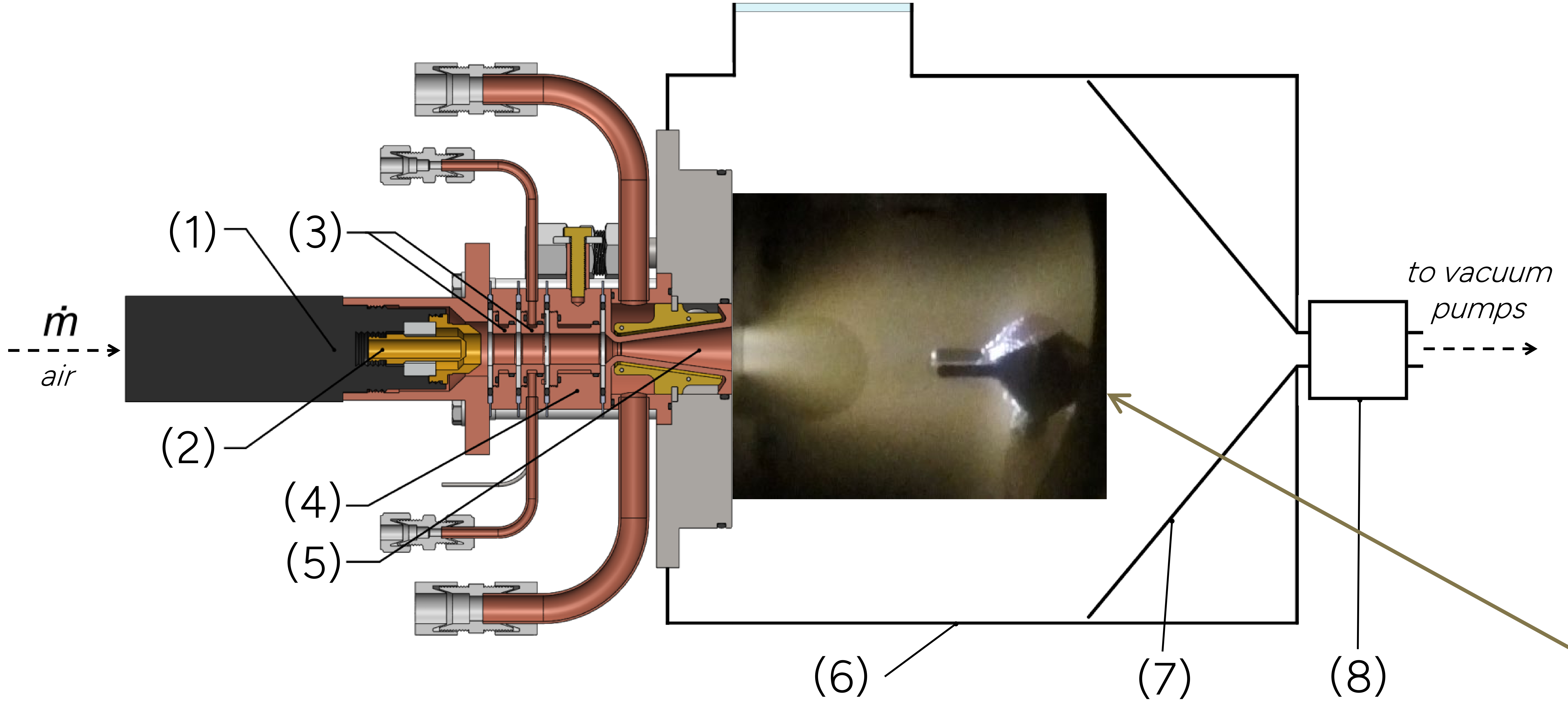

Components:

1. MAX 200 torch body
2. Cathode
3. Constrictor disks (x2)
4. Anode
5. Nozzle
6. Test box
7. Diffuser (*new*)
8. Heat exchanger (*new*)

Cooling circuit 1

Cooling circuit 2

\+ sweep arm for intrusive flow characterization

Facility — flow characterization

Non-intrusive flow diagnostics:

- High-speed camera with notch filter
- Optical emission spectroscopy (OES)

– in progress –

Intrusive flow diagnostics:

- Sweep arm with trident holder
- Water-cooled Gardon gauge (3/16" hemispherical) used for stagnation point heat flux measurements

1 sec dwell

~0.7 m/s sweep speed

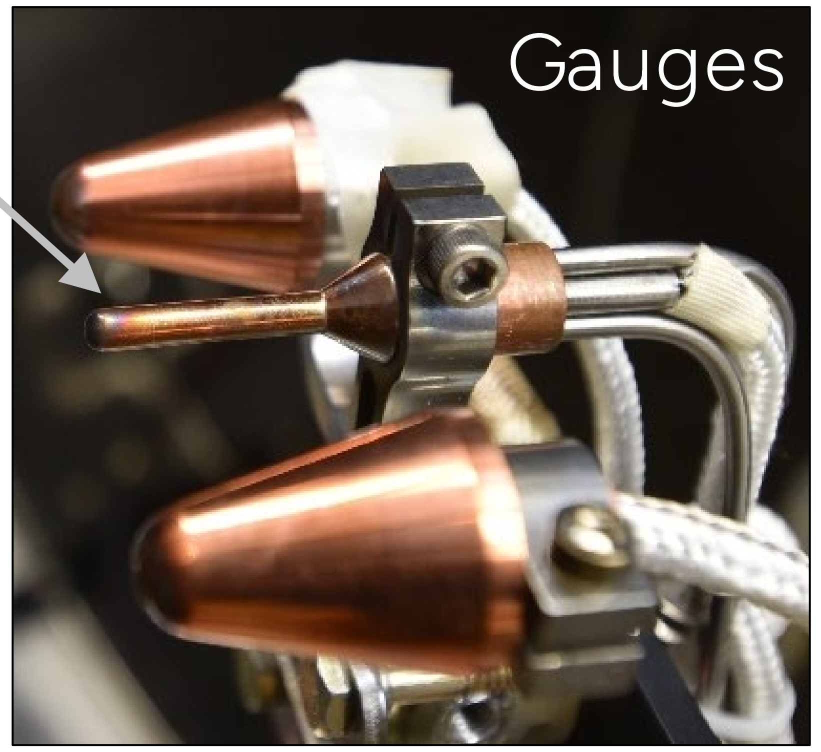

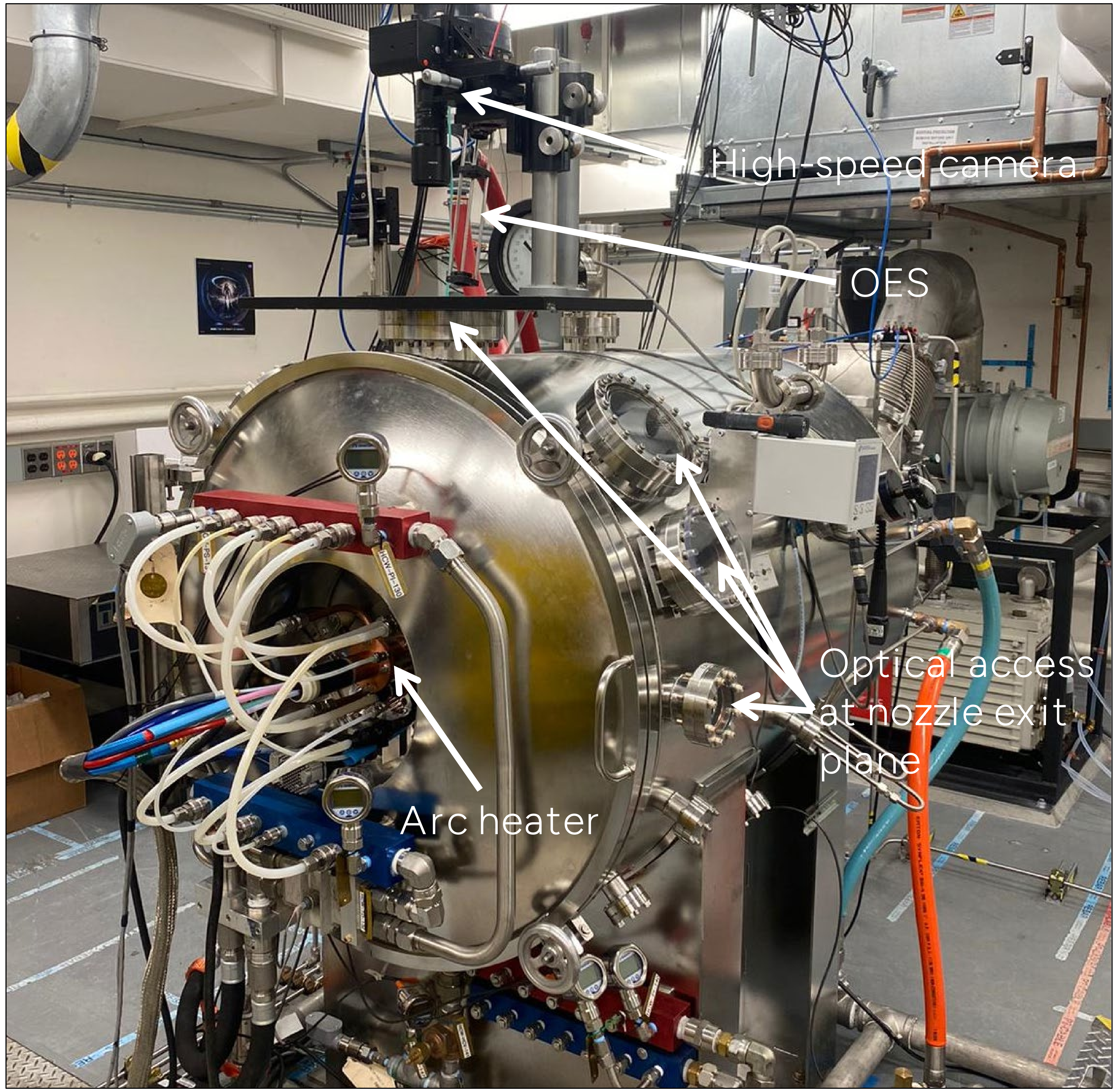

Facility — upgraded vacuum system

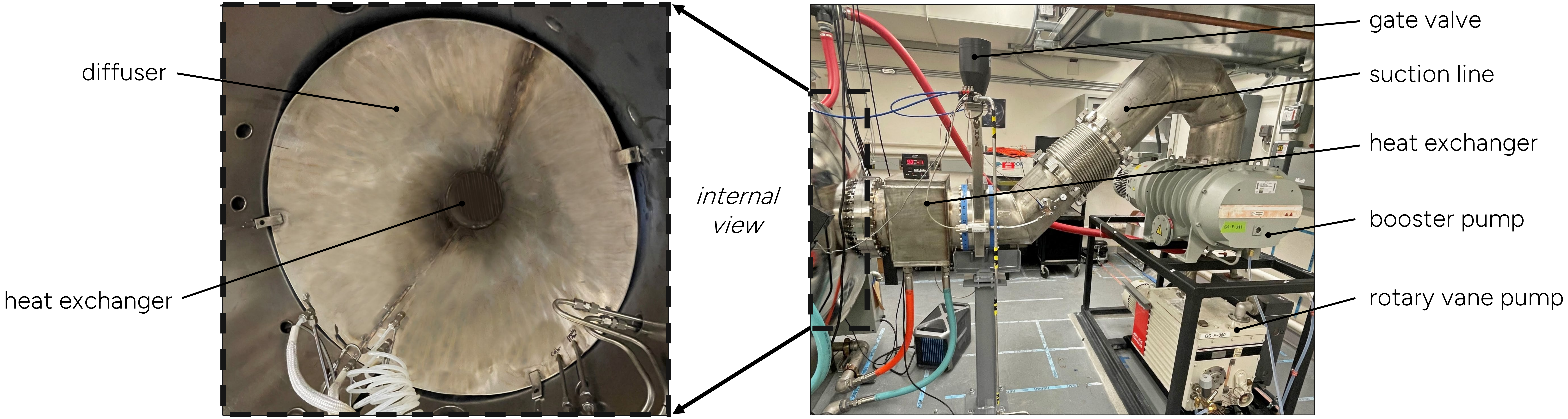

- Refurbished mechanical booster pump was procured and coupled to the existing two-stage direct drive rotary vane pump (both water-cooled).
- Water-cooled diffuser and a heat exchanger were designed in-house and installed.

Arc-jet performance

Flow enthalpy equations & numerical modeling

Flow enthalpy — enthalpy by energy balance (EB^2)

A bulk enthalpy estimate can be calculated via an energy balance from the arc power P_{arc} and the power lost in the arc heater cooling circuit ΔP_{cool}:

$$\bar{h}_{\mathrm{EB2}} = \frac{P_{\mathrm{arc}} - \Delta P_{\mathrm{cool}}}{\dot{m}} = \frac{(IV) - (\dot{m}_{\mathrm{W}} c_{\mathrm{p,W}} \Delta T_{\mathrm{W}})}{\dot{m}}$$

where

I :	arc current
V :	arc voltage
$\dot{m}$:	air mass flow rate
$\dot{m}_{\mathrm{W}}$:	cooling water flow rate
ΔT_{W} :	temperature difference between water supply and return lines
$c_{\mathrm{p,W}}$:	isobaric specific heat capacity (water)

- Commonly used in the high-power arc-jet facilities at NASA Ames.

Flow enthalpy — sonic flow method & correlations

Other formulations are available:

$$\bar{h}^{\mathrm{W}} = \left(\frac{123}{\sigma}\right)^{2.52}$$

Winovich (1964)

$$\bar{h}^{\mathrm{S}} = \left(\frac{158.7}{\sigma}\right)^{1.971}$$

Shepard et al. (1993)

$$\bar{h}^{\mathrm{T}} = \left(\frac{155.8}{\sigma}\right)^{2}$$

Thompson, Prabhu, et al. (2011)

where the sonic flow parameter $\sigma = \dfrac{\dot{m}}{A_t p_{0,\mathrm{col}}}$ [kg/m²atm]

- The correlation constants are known to be facility dependent.

Numerical modeling — laminar Navier–Stokes

Laminar simulations were performed using the Data Parallel Line Relaxation (DPLR) code, v4.04.

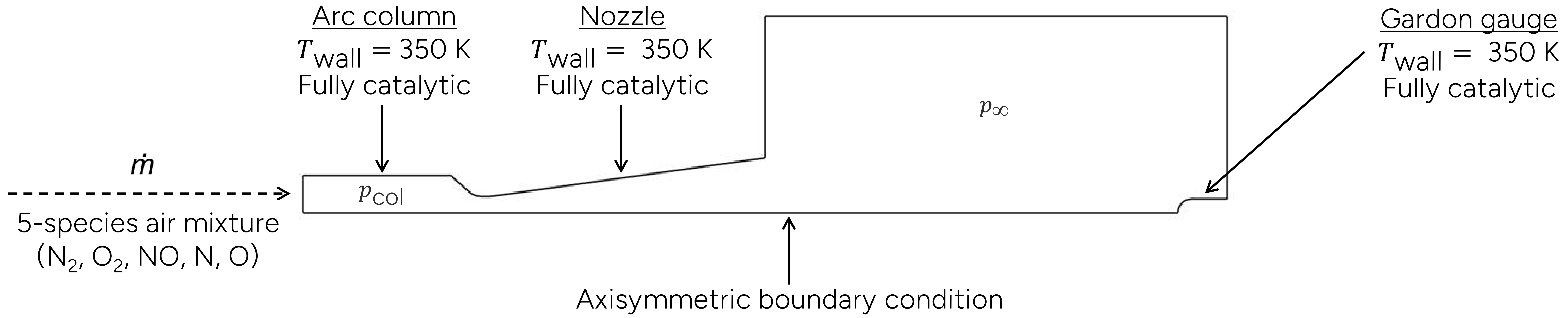

- Experimental measurements for air flow rate $\dot{m}$, arc column pressure p_{col}, and test box pressure p_∞ were combined with chemical equilibrium calculations (CEA) to set the inlet/outlet boundary conditions.
- Inlet enthalpy $\bar{h}$ was calculated using the Winovich equation $\left(\bar{h}^{\text{W}}\right)$.

Test matrix

Seven runs were completed over the course of a two-day Integrated Systems Testing campaign.

Run	Measured arc current I_{arc} [A]	Measured flow rate, $\dot{m}$ [g/s]
1	42	0.23
2	96	0.23
3	142	0.23
4	188	0.23
5	40	0.23
6	183	0.23
7	42	0.14

The Gardon gauge was 70 mm from the nozzle exit plane for all conditions.

Results & Discussion

Performance of the new vacuum system

Before arc-on (pump-down)

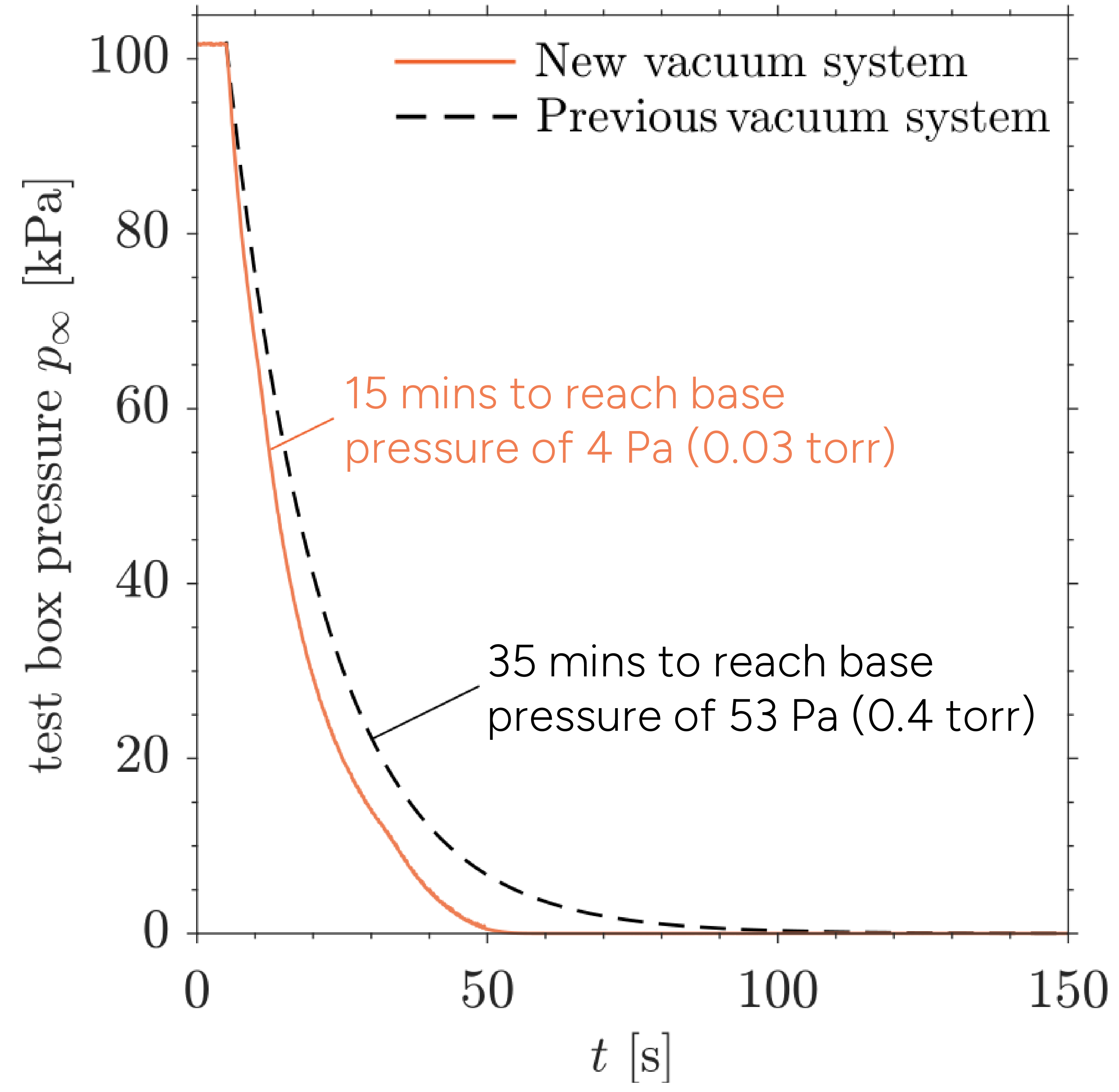

After arc-on (t = 0 s)

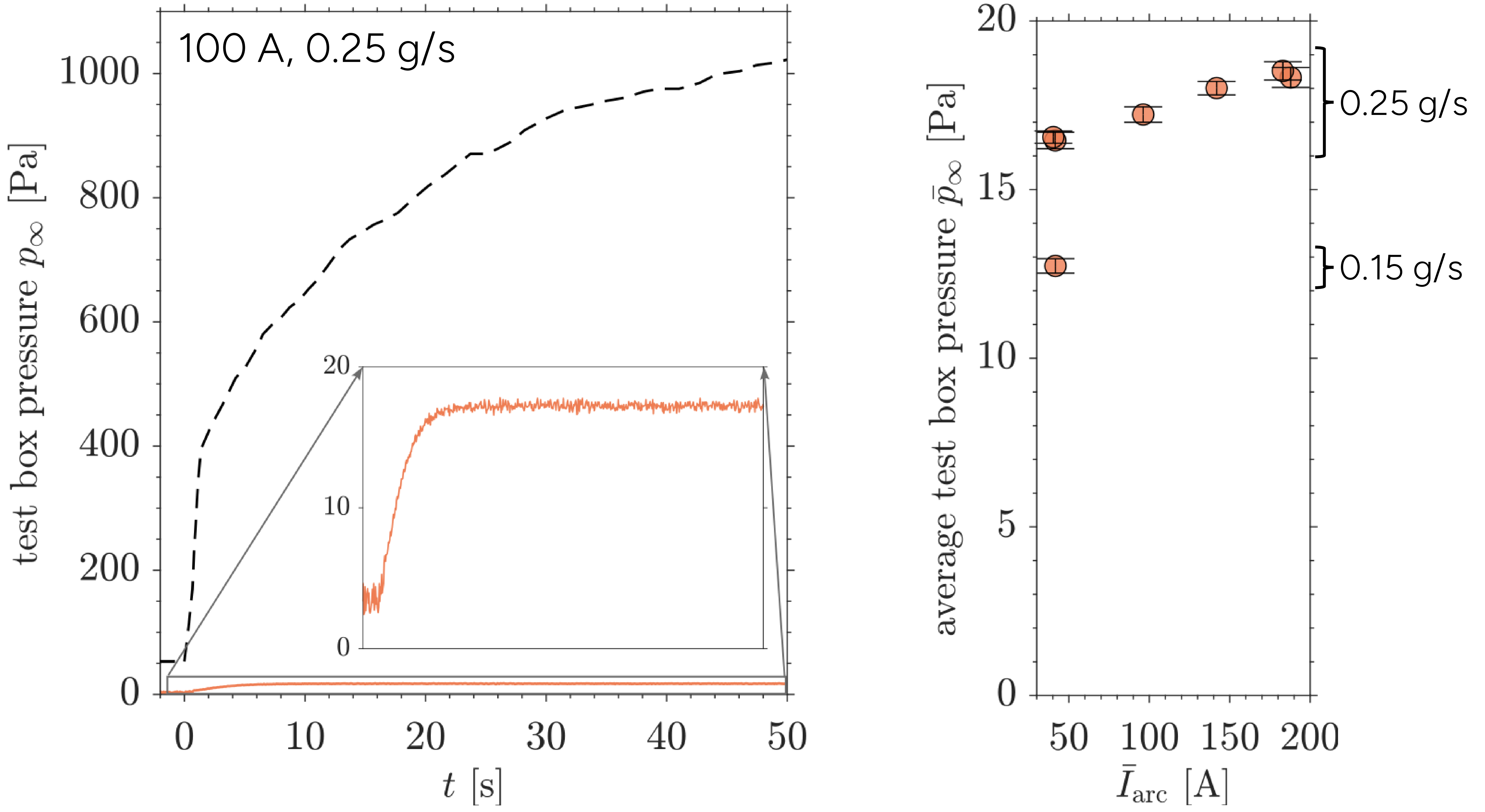

- <u>2X improvement</u> in pump-down time to base pressure, <u>13X improvement</u> in base pressure.
- After arc-on, test box reached steady-state in <u><10 seconds</u> where $p_e/p_\infty>1$.
- Average test box pressure during tests: ~17±0.2 Pa (0.13±0.002 torr).

Performance of the new vacuum system

Change in nozzle flow structure

For the same set conditions: 100 A, 0.25 g/s

Previous vacuum system

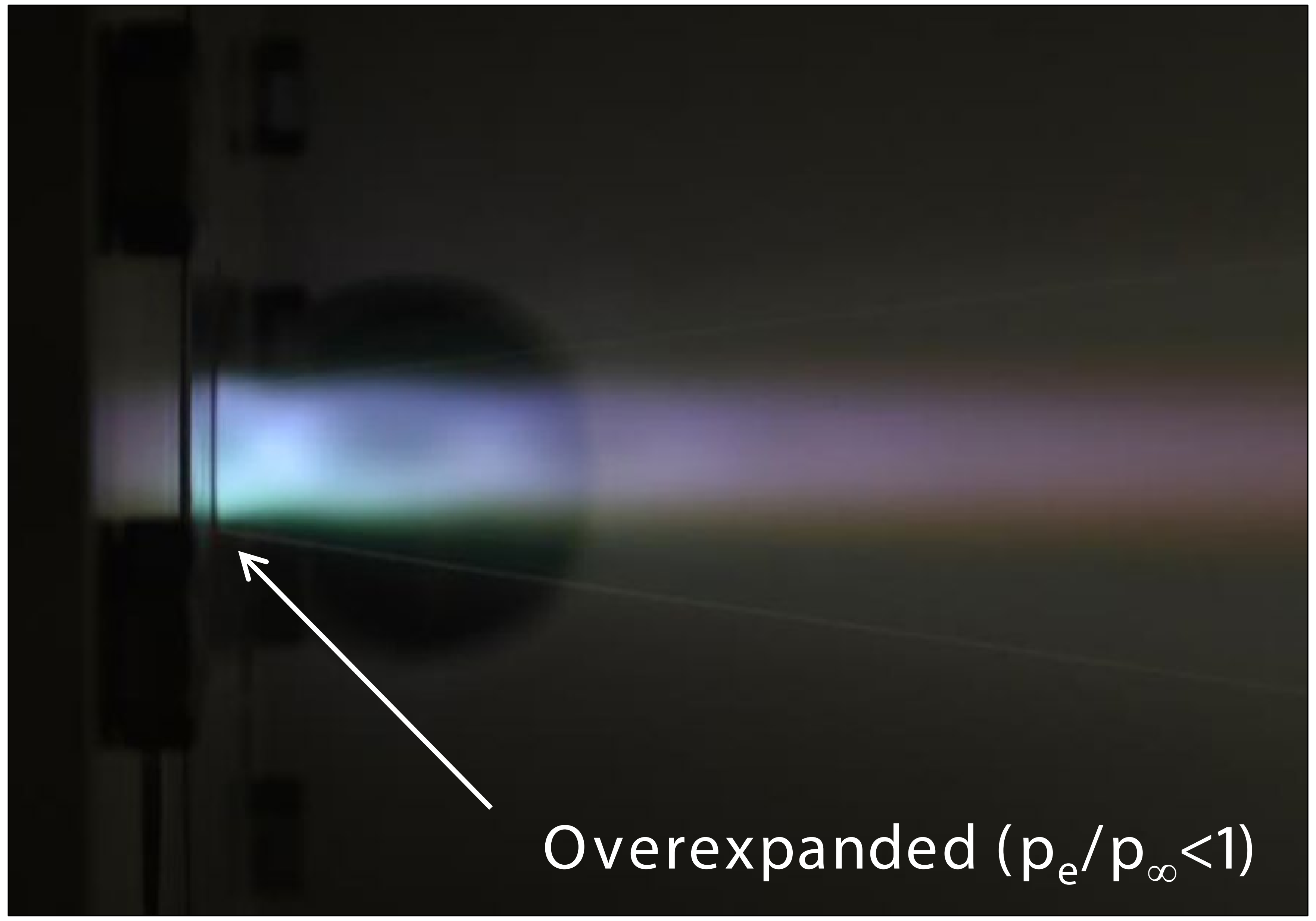

New vacuum system

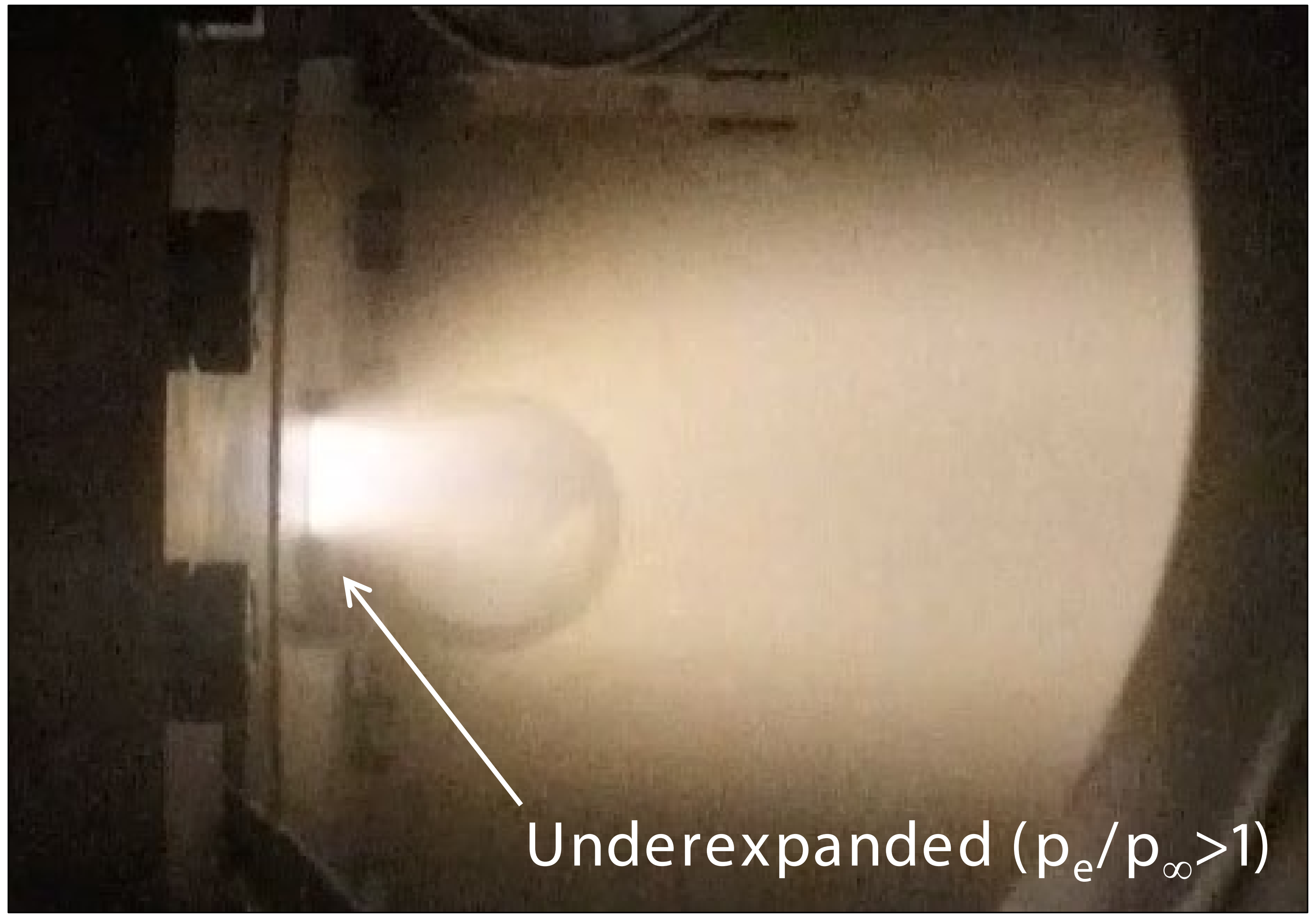

Bulk flow enthalpy

EB² measurements — $\bar{\dot{m}} = 0.23$ g/s

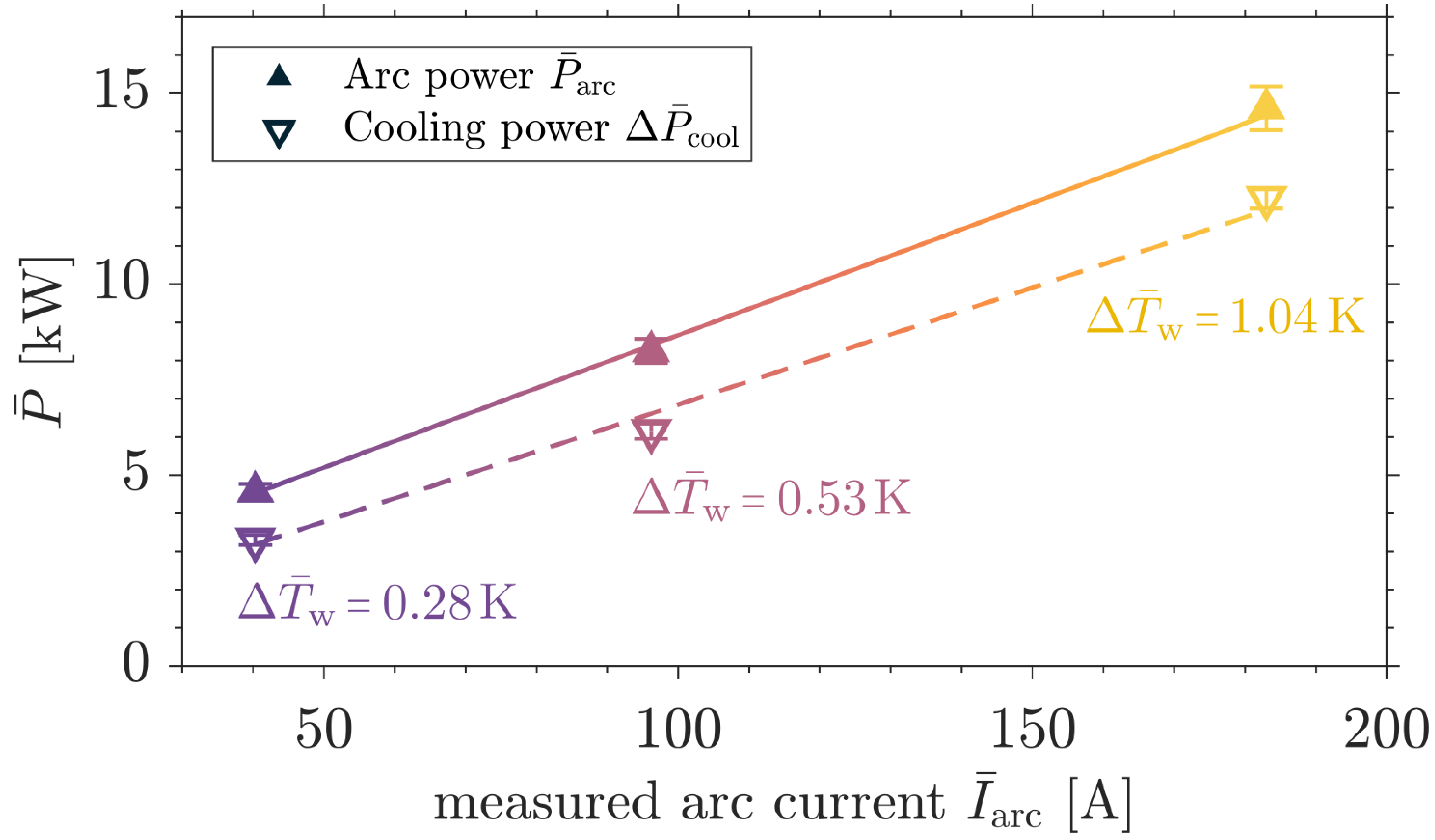

$$\bar{h}_{\mathrm{EB2}} = \frac{P_{\mathrm{arc}} - \Delta P_{\mathrm{cool}}}{\dot{m}} = \frac{7.99\bar{I}_{\mathrm{arc}} + 1018.7}{0.23 \times 10^{-3}}$$

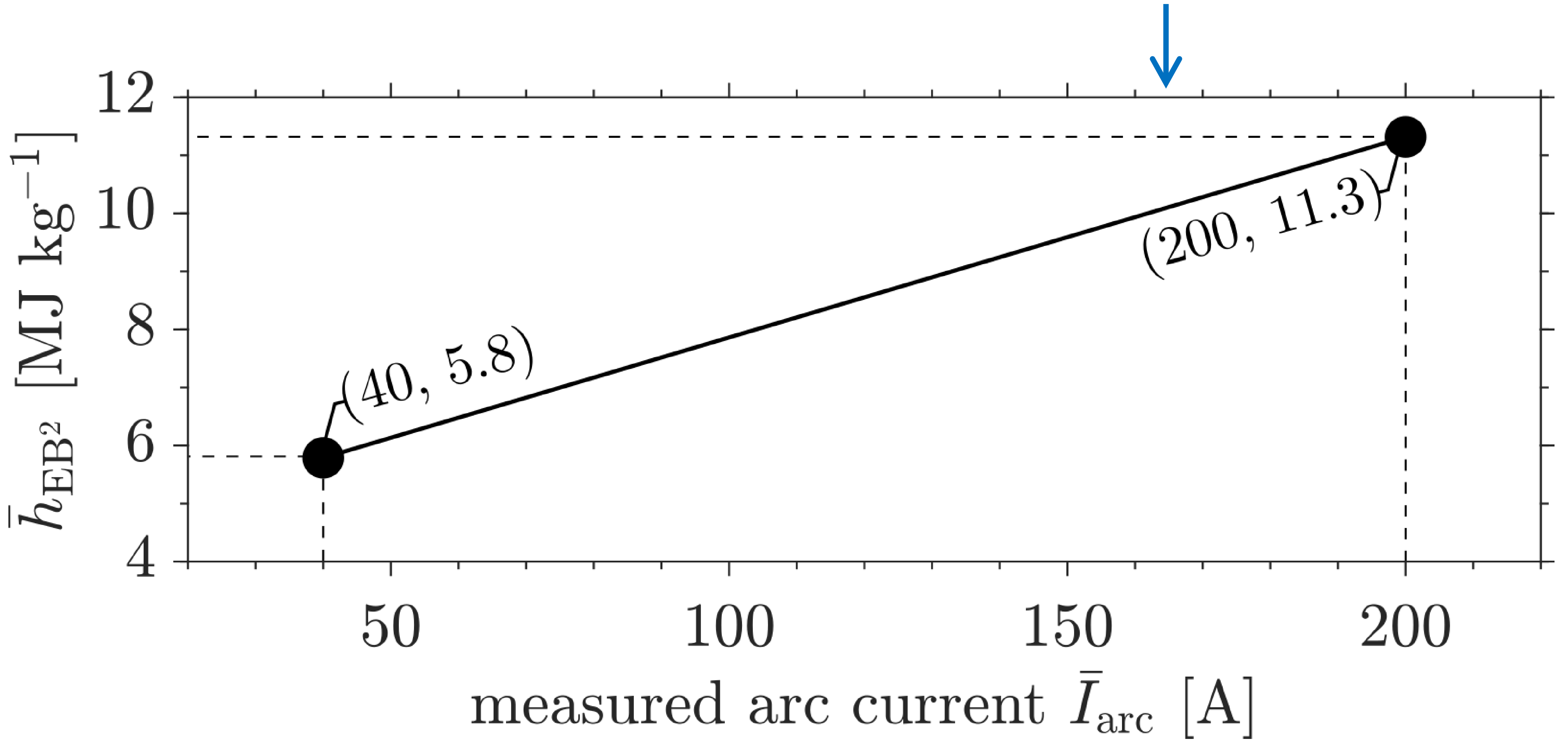

- Despite low ΔT_W values, SNR(ΔT_W) is high: 29 to 85.
- We fit linear polynomials through the arc power P_{arc} and cooling power ΔP_{cool} data points.
- A relationship between I_{arc} and h_{EB2} is proposed for $\bar{\dot{m}}$ = 0.23 g/s: when a specific enthalpy is desired at this flow rate, the required arc current setting can be simply back-calculated.

Bulk flow enthalpy

Comparison with previous mARC datasets

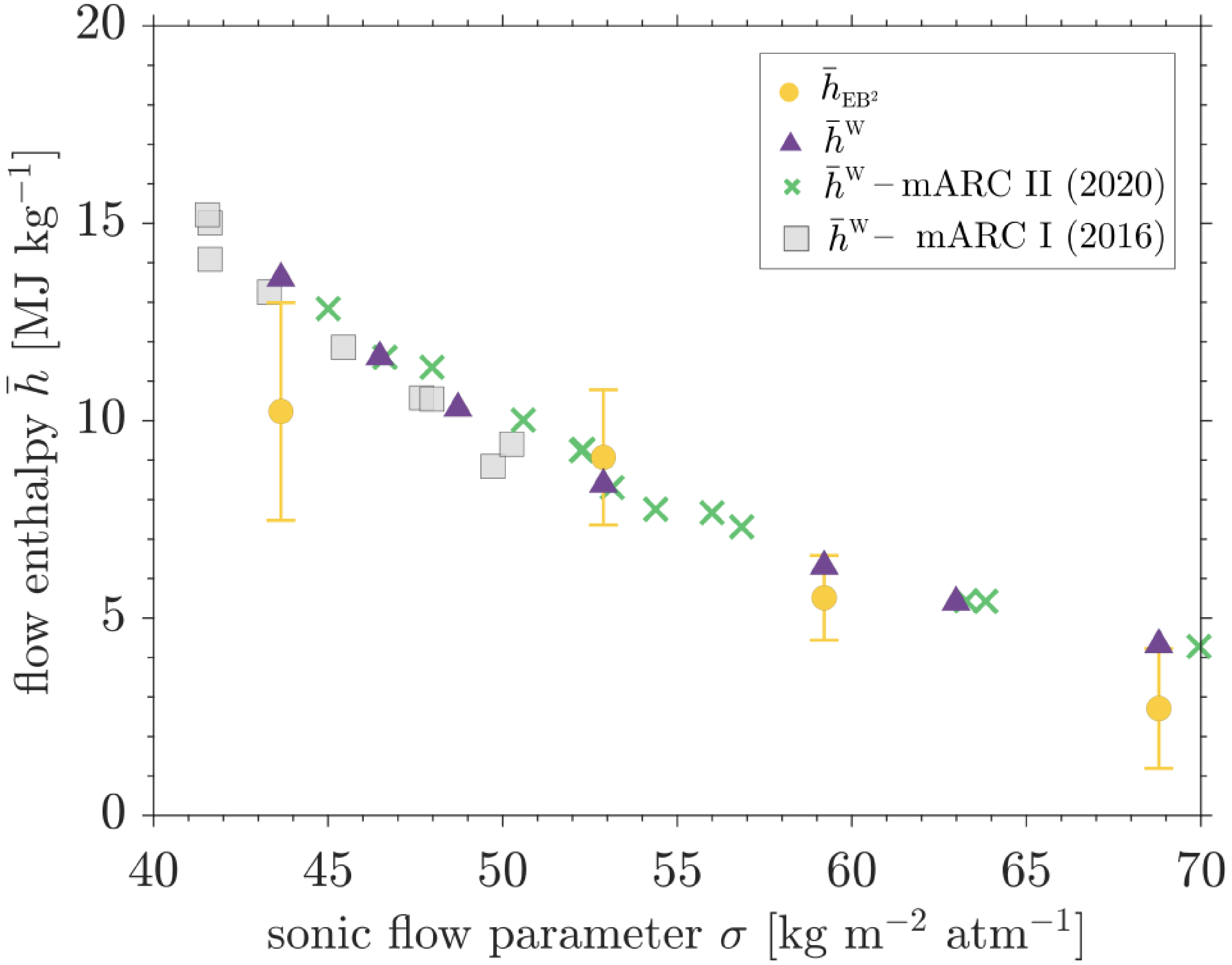

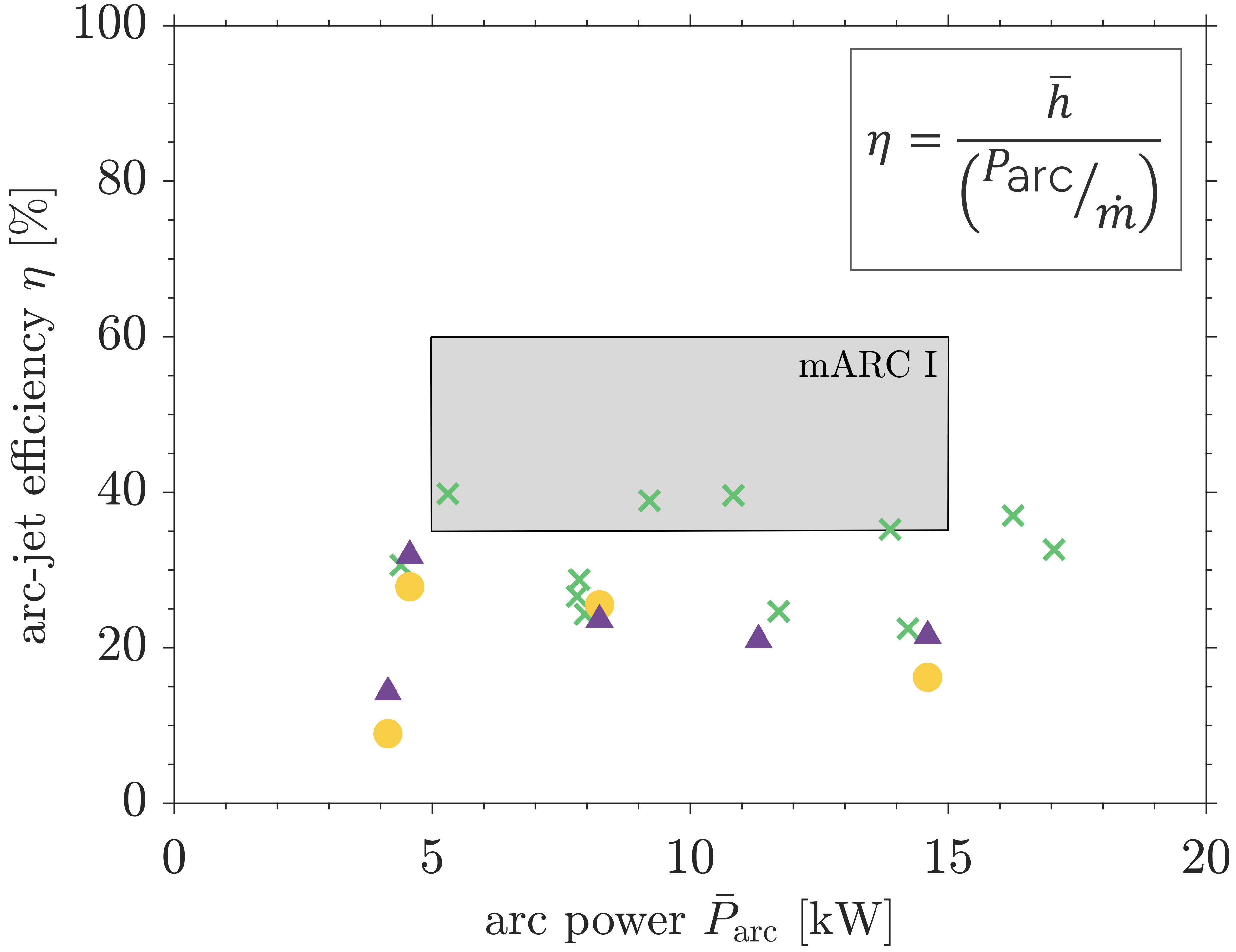

- EB² method: three of the four EB² enthalpy values are lower than those calculated via Winovich.
- Using the Winovich equation, we report arc-jet efficiencies of $14 < \eta < 32\%$.
- Combination of low current and high flow rate leads to highest η.
- Detailed comparison will be possible after full characterization of the facility is completed.

Stagnation point heat flux

3/16" hemispherical Gardon gauge (water-cooled)

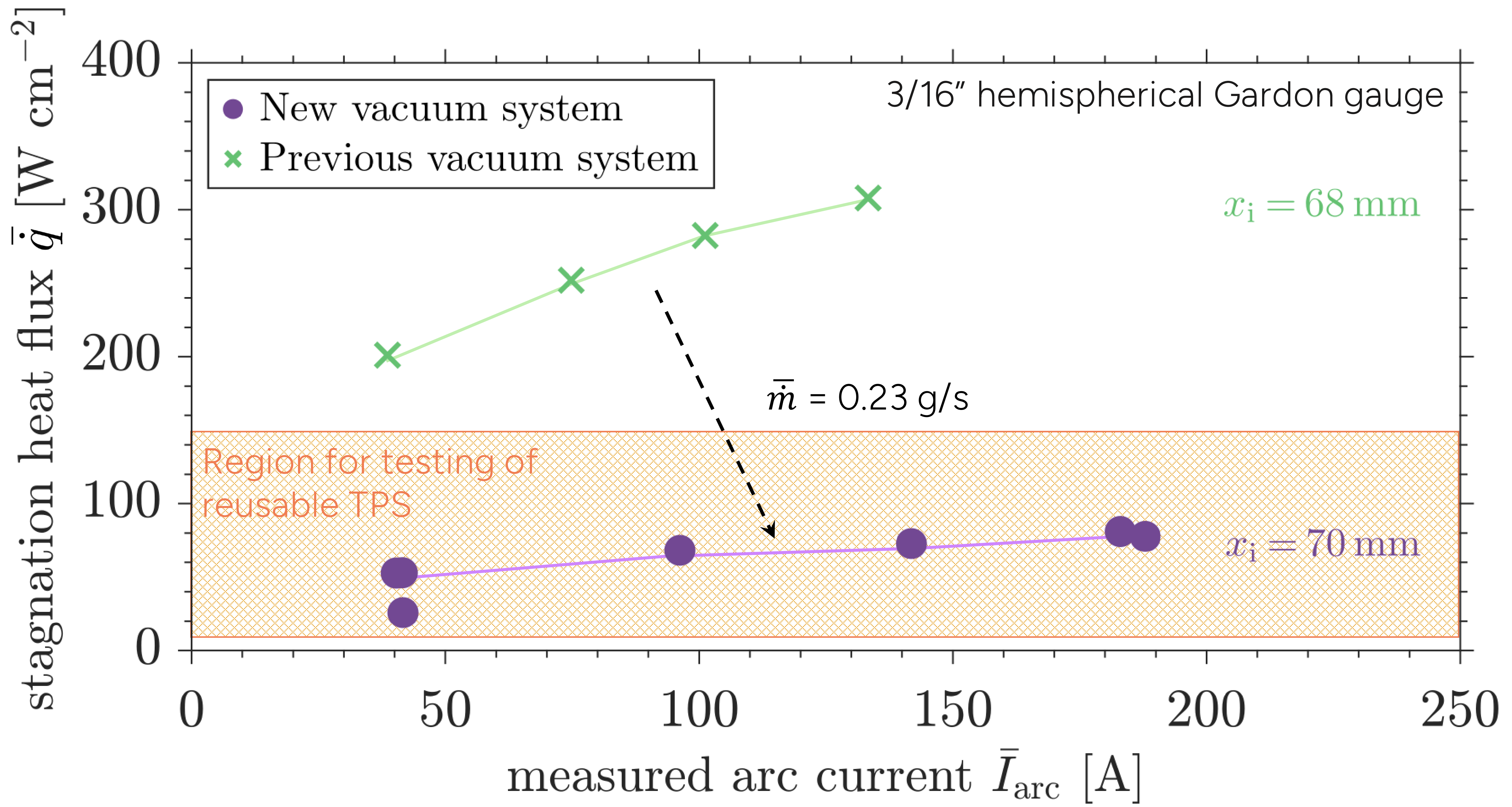

41 A, 0.14 g/s | 40 A, 0.23 g/s | 96 A, 0.23 g/s | 142 A, 0.23 g/s | 183 A, 0.23 g/s

- Upgraded vacuum system has enabled mARC II to generate the desired underexpanded flow (p_e/p_∞>1).
- This has led to a ~4X reduction in heat flux for the same set test conditions.
- We report the lowest stagnation point heat fluxes measured in mARC II to date:
  - minimum of **26 W/cm²**
  - maximum of **81 W/cm²**
  - Can deliver the low heating rates needed for testing of low-maturity tech (e.g., reusable TPS materials).
  - kW/cm² heat fluxes are anticipated for ↑ currents, ↑ flow rates, and ↓ distance from nozzle.

Numerical results

Laminar axisymmetric model (42 A, 0.23 g/s)

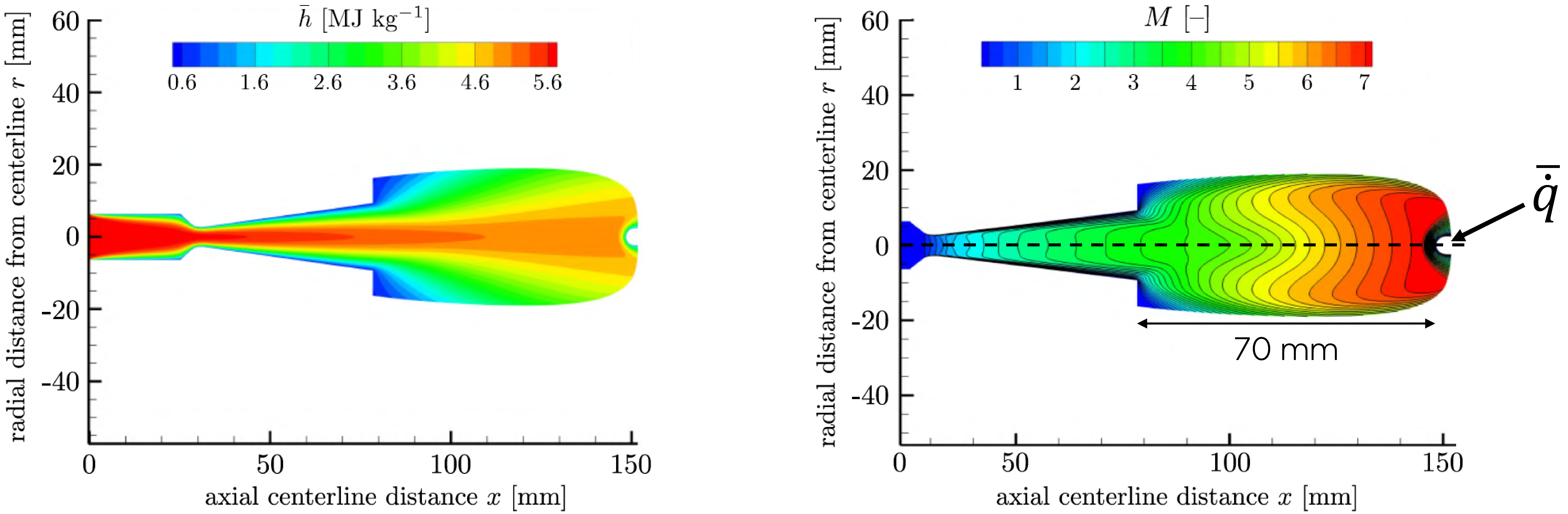

- Radial enthalpy gradient is steep near the walls owing to heat conduction (T_W = 350 K).
- No visible Mach disk upstream of Gardon gauge for conditions tested in present work*.

*Franquet et al., 'Free underexpanded jets in a quiescent medium: A review' (2015).

Numerical results

Stagnation point heat flux — comparing to experimental data

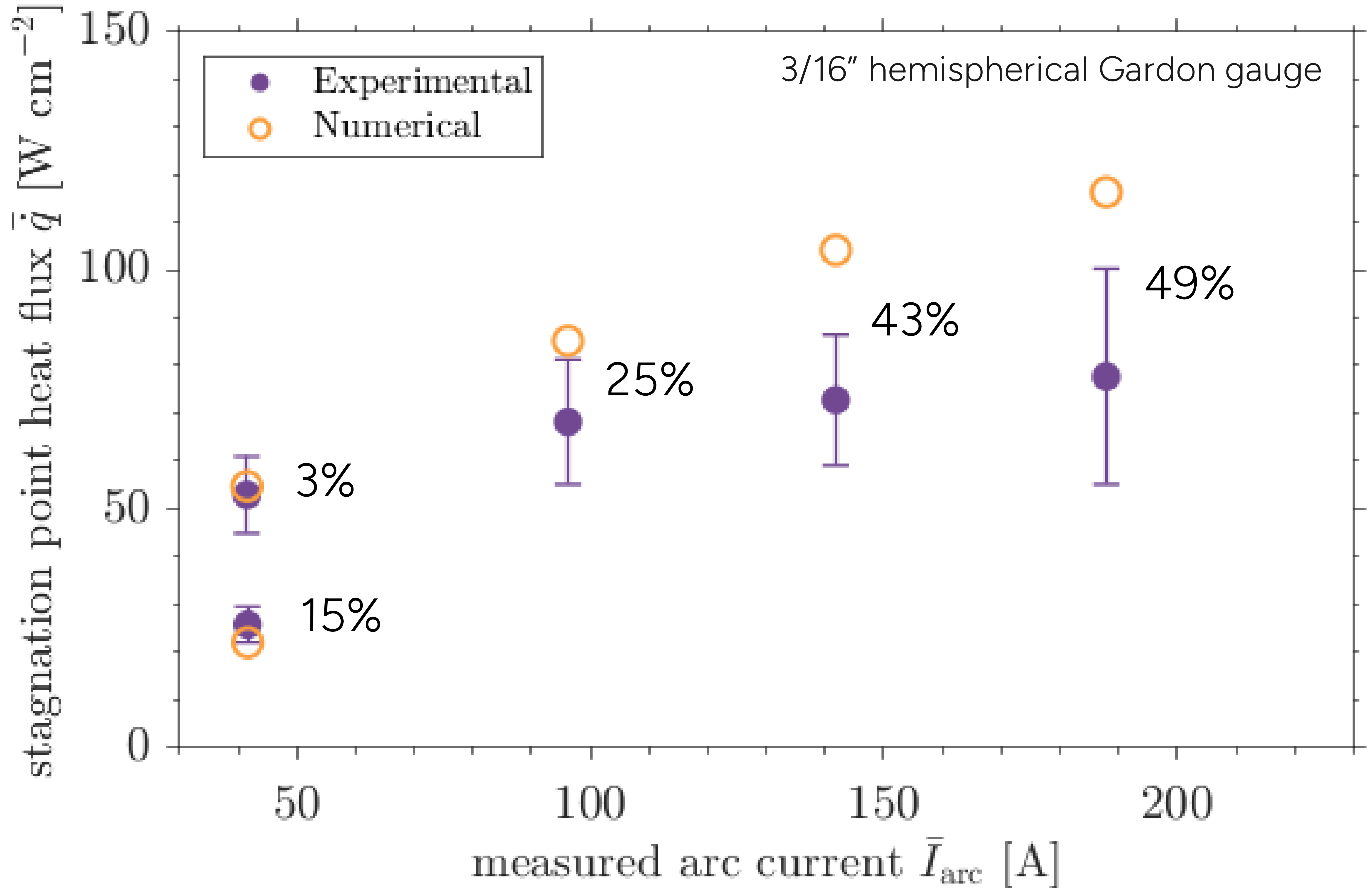

- Laminar model shows good agreement with experimental results at low arc currents (3–15%, 42 A).
- Discrepancy between experimental measurements and numerical results increases with arc power (49%, 188 A).
- Further work will be undertaken to understand the reasons behind this trend.

Concluding Remarks & Future Work

Concluding Remarks

Integrated Systems Testing campaign was completed after the mARC II facility was upgraded.

1. The vacuum system upgrade had a significant impact on mARC II performance:

- 13X improvement in base pressure pre-test & reliable underexpanded flow ($p_e/p_\infty > 1$) during test.
- Reduced heat fluxes by ~4X for same set test conditions.
- Lowest heat fluxes measured in mARC II to date (26–81 W/cm^2).
- First demonstration that mARC II can enable research needing low heat rate testing.

Concluding Remarks

Integrated Systems Testing campaign was completed after the mARC II facility was upgraded.

2. Bulk enthalpy via EB^2 method was reported for the first time for mARC II:

- Initial data suggests EB^2 generally estimates lower enthalpy than sonic flow (e.g., Winovich).
- Simple equation is proposed for interpolating EB^2 enthalpy based on arc current ($\dot{m}$ = 0.23 g/s).

3. Laminar numerical simulations were undertaken:

- Good agreement with experimental stagnation point heat flux at low arc currents (3–15%, 42 A).
- Discrepancy increases with arc power (49%, 188 A).

Future Work

1. Full characterization of mARC II's operational envelope of using air flows will be completed:
   - Stagnation heat flux, radial heat flux profile, and stagnation pressure.
   - EB^2 enthalpy to develop a correlation for the mARC II facility.

2. Additional efforts will be undertaken to understand the disparity between experimental and numerical heat flux results at higher set arc currents.

3. Optical diagnostics have been implemented to characterize species and shock structures in the flow — further refinements and expansions planned.

Acknowledgements

Funding:

- J. Rodrigues is the recipient of a NASA Postdoctoral Program (NPP) research fellowship at NASA Ames Research Center, administered by Oak Ridge Associated Universities (ORAU) under contract with NASA.
- S. Colom is supported through the NASA NNA15BB15C contract.
- R. Chung and J. Hartman are supported through the NASA 80ARC022DA011 contract.

Design & fabrication:

- James Hope, Rommel Mallorca, Matthew Hoffer, Juan Tapia, Alejandro Contreras, Pedro Solano, Nicholas Reed, Jacob Weiland, Richard Ryzinga, and Casey Ching for supporting the facility upgrades.
- Andrew Morgan (NSWCDD Reentry Systems Office) for help with the design and analysis of the vacuum system upgrade.

for the benefit of all

References

1. Karl, S., and Bykerk, T., “Sustainable space technologies—Strategies toward a predictive aerothermal design of re-useable space transportation systems,” Review of Scientific Instruments, Vol. 95, No. 2, 2024.
2. MacDonald, M. E., Balboni, J., Cornelison, C., Hartman, J., Haw, M., Fretter, E., Cruden, B., Wilder, M., and Hwang, H., “NASA Ames Thermophysics Ground Test Facilities Supporting Future Planetary Atmospheric Entry,” Bulletin of the AAS, Vol. 53, No. 4, 2021.
3. Lundell, J. H., Otten, L. J., and Dickey, R. R., “The CO_2 gasdynamic laser as a high-intensity radiation facility,” 13th Aerospace Sciences Meeting, AIAA, 1975.
4. Winovich, W., and Carlson, W. C. A., “The 60-MW Shuttle Interaction Heating Facility,” Proceedings of the 25th International Instrumentation Symposium, ISA, 1979.
5. Balter-Peterson, A., Nichols, F., Mifsud, B., and Love, W., “Arc jet testing in NASA Ames Research Center thermophysics facilities,” AIAA 4th International Aerospace Planes Conference, 1992.
6. Wilder, M. C., Bogdanoff, D. W., and Cornelison, C. J., “Hypersonic Testing Capabilities at the NASA Ames Ballistic Ranges,” 53rd AIAA Aerospace Sciences Meeting, AIAA, 2015.
7. Cushman, G., Alunni, A., Balboni, J., Zell, P., Hartman, J., and Empey, D., “The Laser Enhanced Arc-Jet Facility (LEAF-Lite): Simulating Convective and Radiative Heating with Arc-jets and Multiple 50-kW CW Lasers,” 2018 Joint Thermophysics and Heat Transfer Conference, AIAA, 2018.
8. MacDonald, M., Rodrigues, J., Cushman, G., Martin, K., and Hartman, J., “Simultaneous Convective and Radiative Heating of Materials with the 200 kW Laser Enhanced Arc Jet Facility (LEAF),” NSMMS & CRASTE Joint Symposia, 2023.
9. Calomino, A., Bruce, W., Gage, P., Horn, D., Mastaler, M., Rigali, D., Robey, J., Voss, L., Wahlberg, J., and Williams, C., “Evaluation of the NASA Arc Jet Capabilities to Support Mission Requirements [NASA/SP-2010-577],” Office of the Chief Engineer, 2010.
10. Terrazas-Salinas, I., “Test Planning Guide for NASA Ames Research Center Arc Jet Complex and Range Complex [A029-9701- XM3 Rev. J – July 28, 2022],” NASA Ames Research Center, 2022.
11. Fu, J., Olivares, R., Oishi, T., Martinez, E., and Gorbunov, S., “XJet: A Small-Scale Aerothermal Test Environment for Instrumentation,” 44th AIAA Aerospace Sciences Meeting and Exhibit, AIAA, 2006.
12. Beck, R. A., White, S., Arnold, J., Fan, W., Stackpoole, M., Agrawal, P., and Coughlin, S., “Overview of Initial Development of Flexible Ablators for Hypersonic Inflatable Aerodynamic Decelerators,” 21st AIAA Aerodynamic Decelerator Systems Technology Conference and Seminar, AIAA, 2011.
13. Fan, W., Thornton, J., Chavez-Garcia, J., Beck, R., and Ghandehari, E., “Charring Behavior of Lightweight Silicone-based Ablators,” 43rd AIAA Thermophysics Conference, AIAA, 2012.
14. White, S., “Effects of Laser Wavelength on Ablator Testing,” 38th Annual Conference on Composites, Materials and Structures, No. ARC-E-DAA-TN12788, 2014.
15. Codron, D. A., and Nawaz, A., “Radial Profiles of Plasma Electron Characteristics in a 30 kW Arc Jet,” 44th AIAA Plasmadynamics and Lasers Conference, AIAA, 2013.

References

16. Codron, D. A., Cruden, B. A., and Ho, T., “Emission Spectroscopy Characterization of Thermal Protection System Materials in Arc-Heated Flows,” 45th AIAA Plasmadynamics and Lasers Conference, AIAA, 2014.
17. Nawaz, A., Ho, T. S., Philippidis, D., MacDonald, M., McGlaughlin, M. S., and Driver, D. M., “Baseline characterization of the 30 kW miniature arc jet facility mARC at NASA Ames,” 32nd AIAA Aerodynamic Measurement Technology and Ground Testing Conference, AIAA, 2016.
18. MacDonald, M. E., Philippidis, D., Ho, T., Haw, M., Hartman, J., and McGlaughlin, M., “Build-up of the second- generation 30 kW miniature arc jet (mARC II) at NASA Ames Research Center,” AIAA Aviation 2019 FORUM, AIAA, 2019.
19. MacDonald, M. E., Philippidis, D., Haw, M., Schickele, D., Luis, D., Hartman, J., and McGlaughlin, M., “Initial Characterization of the 30 kW Miniature Arc Jet (mARC II) at NASA Ames Research Center,” AIAA AVIATION 2020 FORUM, AIAA, 2020.
20. Luís, D., and MacDonald, M. E., “Emission spectroscopy characterization of electrode species in the freestream flow at the NASA Ames miniature Arc Jet II facility,” Journal of Quantitative Spectroscopy and Radiative Transfer, Vol. 272, 2021.
21. MacDonald, M. E., Haw, M. A., Martinez, R., Colom, S., Rodrigues, J., Chung, R., and Hartman, J., “Characterizing Heat Flux in the miniature Arc jet Research Chamber (mARC II),” AIAA AVIATION 2023 FORUM, AIAA, 2023.
22. Haw, M. A., MacDonald, M. E., and Colom, S. V., “Big-data Efficient and Automated Science Transfer (BEAST): an open-source software architecture for arc jet data management, modeling, and automation,” AIAA SCITECH 2023 Forum, AIAA, 2023.
23. ASTM International, “Standard Practice for Measuring Plasma Arc Gas Enthalpy by Energy Balance [ASTM E341–08],” ASTM International, 2020.
24. Hightower, T. M., Balboni, J. A., MacDonald, C. L., Anderson, K. F., and Martinez, E. R., “Enthalpy by energy balance for aerodynamic heating facility at NASA Ames Research Center Arc Jet Complex,” 48th International Instrumentation Symposium, ISA, 2002.
25. Thompson, C., Prabhu, D., Terrazas-Salinas, I., and Mach, J., “Bulk Enthalpy Calculations in the Arc Jet Facility at NASA ARC,” 42nd AIAA Thermophysics Conference, AIAA, 2011.
26. Winovich, W., “On the equilibrium sonic-flow method for evaluating electric-arc air-heater performance (NASA TN D-2132),” NASA Ames Research Center, 1964.
27. Shepard, C., Milos, F., and Taunk, J., “A sonic flow equation for electric arc jets,” 24th Plasma Dynamics, and Lasers Conference, AIAA, 1993.
28. Wright, M. J., White, T., and Mangini, N., “Data Parallel Line Relaxation (DPLR) Code User Manual Acadia-Version 4.01.1,” NASA, 2009.
29. Gordon, S., and McBridge, B. J., “Computer Program for Calculation Complex Chemical Equilibrium Compositions and Applications,” NASA Reference Publication 1311, 1996.
30. Park, C., Nonequilibrium Hypersonic Aerothermodynamics, Wiley, 1990.
31. Park, C., “Review of chemical-kinetic problems of future NASA missions. I - Earth entries,” Journal of Thermophysics and Heat Transfer, Vol. 7, No. 3, 1993.

Auxiliary Slides

Bulk flow enthalpy

EB² measurements — $\Delta\bar{T}_W$ time series signals

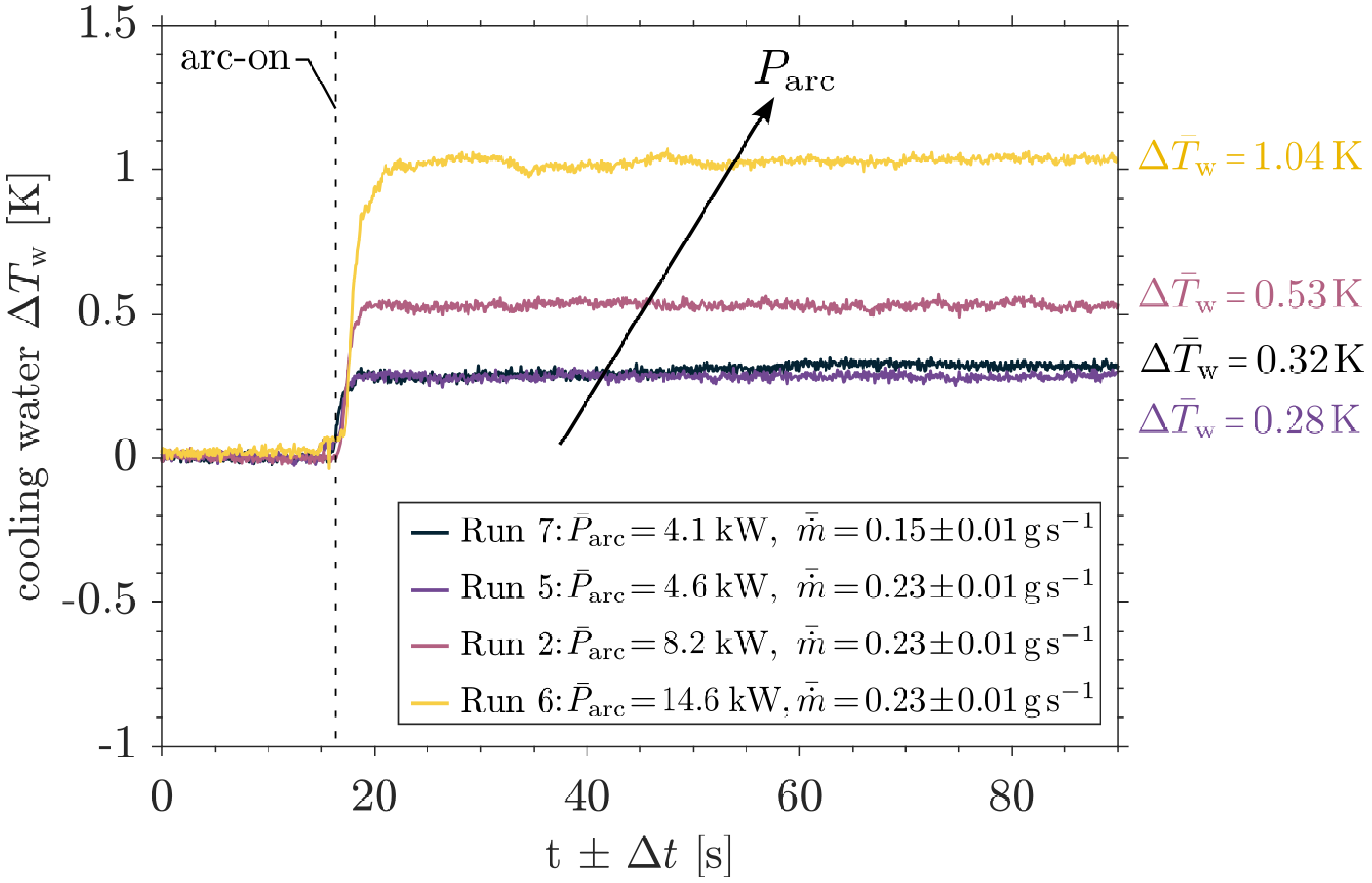

- EB² method is driven by the <u>cooling water flow rate</u> and the <u>temperature change</u> ΔT_W.
- Since water flow rate was measured to be constant ($\bar{\dot{m}}_W$ = 2.79±0.05 kg/s), we plot the cooling water temperature change with time.
- Signals have been shifted in time so that arc-on times align.
- Despite low ΔT_W values, <u>SNR(ΔT_W) is high</u>: 29 to 85.

Stagnation point heat flux

Signal-to-noise in Gardon gauge — 40 A, $\bar{\dot{m}} = 0.23$ g/s

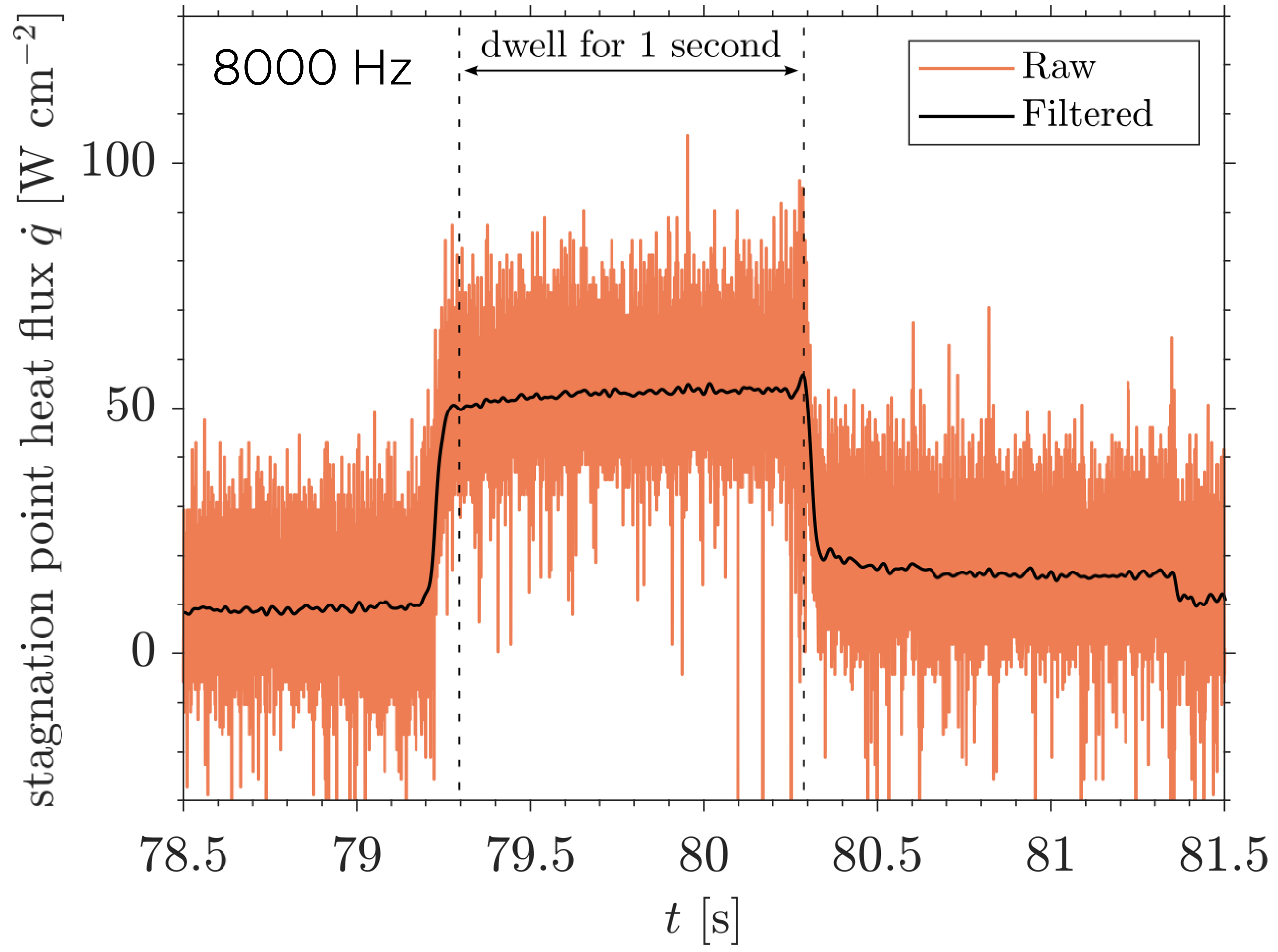

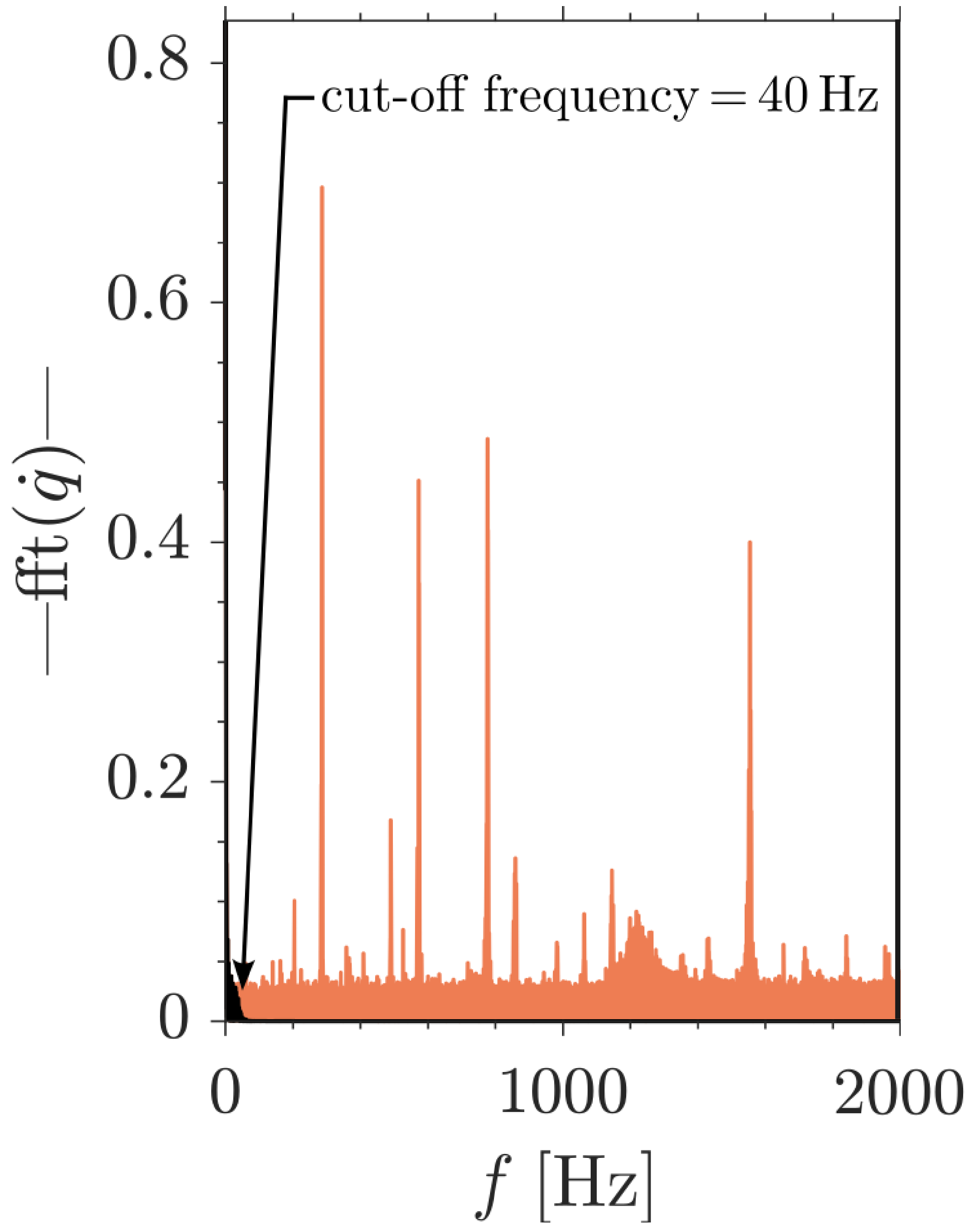

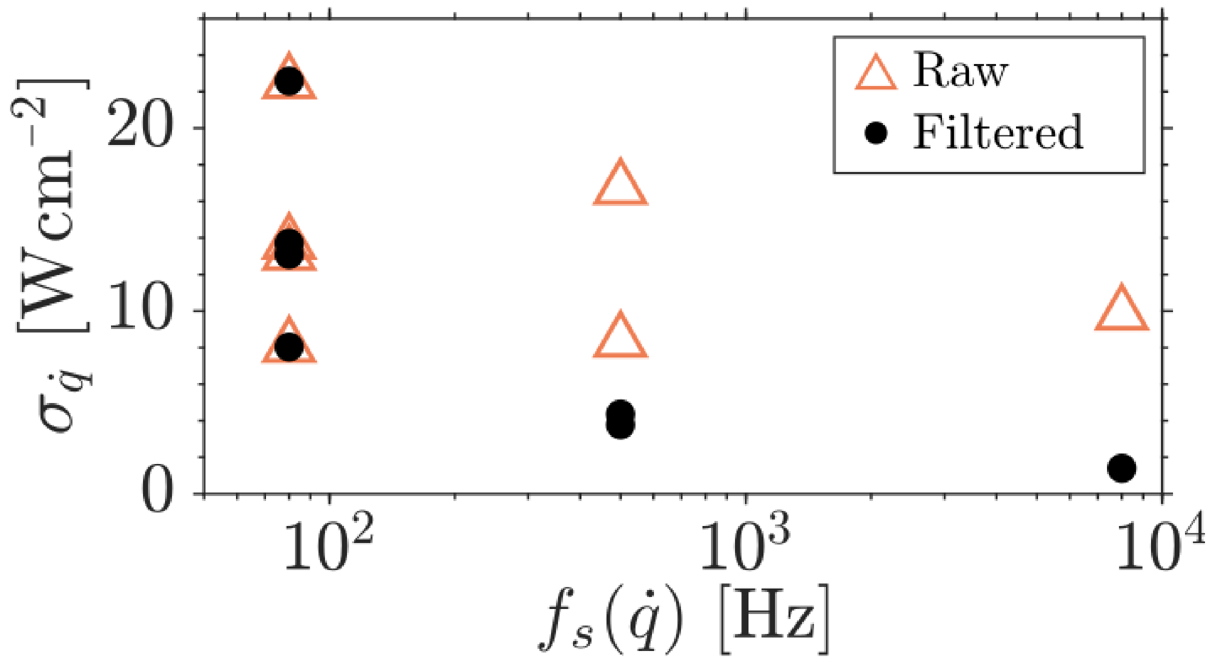

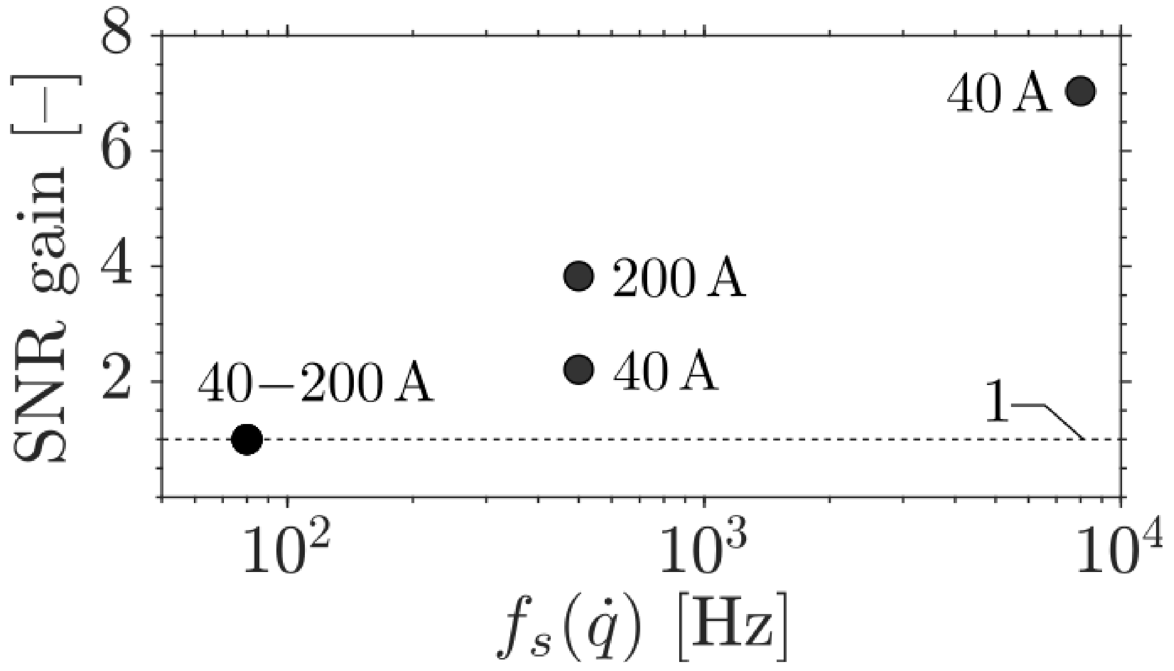

- We sampled at f_s=80 Hz, 500 Hz, and 8000 Hz, depending on the run.
- Four major peaks in the FFT: 300 Hz, 600 Hz, 800 Hz, and 1600 Hz (600 Hz and 1600 Hz are likely 2nd harmonics).
- Low-pass Butterworth filter used to filter higher frequency noise (AC signals not of interest; rise time of raw signal was matched).
- Filtering does not reduce σ or SNR of signal when f_s=80 Hz, but does at f_s=500 Hz and f_s=8000 Hz.
- In future experiments, we will use the highest sampling rate (8000 Hz is currently the maximum) along with the low-pass filter to maximize the SNR of the heat flux measurements.

Test matrix and outputs

Run	Arc column							Operational envelope (two constrictor disks)								DPLR CFD	
	$\dot{m}_{\mathrm{set}}$ [g s^{-1}]	I_{set} [A]	Arc-on [-]	$\bar{\dot{m}}$ [g s^{-1}]	$\bar{I}_{\mathrm{arc}}$ [A]	$\bar{P}_{\mathrm{arc}}$ [kW]	$\bar{p}_{\mathrm{col}}$ [kPa]	$\bar{p}_{\infty}$ [Pa]	x_{i} [mm]	$\bar{\dot{q}}$ [W cm^{-2}]	SNR($\bar{\dot{q}}$) [–]	$f_s(\dot{q})$ [Hz]	$\bar{h}^{\mathrm{W}}$ [MJ kg^{-1}]	$\bar{h}_{\mathrm{EB^2}}$	η [%]	$\bar{\dot{q}}$ [W cm^{-2}]	$\lvert\delta\bar{\dot{q}}\rvert$ [%]
1	0.25	40	✓	0.23	42	–	15	16	70	53	6.6	80	5.4	–	–	55	3%
2	0.25	100	✓	0.23	96	8.2	18	17	70	68	5.2	80	8.4	9.1	24	85	25%
3	0.25	150	✓	0.23	142	11	20	18	70	73	5.3	80	10.3	–	21	104	43%
4	0.25	200	✓	0.23	188	–	21	18	70	78	3.4	80	11.6	–	–	116	49%
5	0.25	40	✓	0.23	40	4.6	16	17	70	53	38	8000	6.3	5.5	32	–	–
6	0.25	200	✓	0.23	183	15	22	19	70	81	19	500	13.6	10	22	–	–
7	0.15	40	✓	0.14	42	4.1	8.3	13	70	26	6.8	500	4.3	2.7	14	22	15%